Materials Research Bulletin 143 (2021) 111443

Contents lists available at ScienceDirect

Materials Research Bulletin

journal homepage: www.elsevier.com/locate/matresbu

Twinned growth of ScN thin films on lattice-matched GaN substrates

Shashidhara Acharya [1,2], Abhijit Chatterjee [1,2], Vijay Bhatia [3], Ashalatha Indiradevi Kamalasanan Pillai [3], Magnus Garbrecht [3], Bivas Saha [1,2,4,*]

[1] Chemistry and Physics of Materials Unit, Jawaharlal Nehru Centre for Advanced Scientific Research, Bangalore 560064, India
[2] International Centre for Materials Science, Jawaharlal Nehru Centre for Advanced Scientific Research, Bangalore 560064, India
[3] Australian Centre for Microscopy and Microanalysis, The University of Sydney, Camperdown, NSW 2006, Australia
[4] School of Advanced Materials (SAMat), Jawaharlal Nehru Centre for Advanced Scientific Research, Bangalore 560064, India

ARTICLE INFO

Keywords:
A. (111) ScN
B. sputtering
C. pole-figure
C. HR(S)TEM
D. rotational twin domains

ABSTRACT

Scandium nitride (ScN) has attracted significant interest in recent years for diverse electronic and thermoelectric applications. Most ScN growth utilizes MgO and Al_2O_3 as substrates that lead to extended defects such as dislocations and grain boundaries. (0001) GaN exhibits less than 0.1% lattice mismatch with (111) ScN, and therefore, should result in single-crystalline ScN film growth. However, not much attention is devoted to understanding the microstructure of ScN on GaN substrates. In this work, we present (111) oriented lattice matched ScN film growth on (0001) GaN substrates. X-ray pole figure exhibited six spots for the (002) ScN superimposed on that of (101) GaN separated by 60° corresponding to twin domains of threefold symmetry for (111) ScN, which are furthermore directly imaged by lattice resolved microscopy images. The presence of twins is attributed to vertical dislocations originating at the GaN/Al_2O_3 interface and extending throughout the GaN film to its interface with ScN.

1. Introduction

In recent years transition metal nitrides (TMN) that are traditionally used as protective layers, hard coatings and tribological applications [1, 2], have garnered significant interest for their electronic, optical and thermoelectric properties [3]. While most of the TMNs are metallic in nature that led to studies on their high-temperature plasmonic applications [4,5], ScN is an ambient-stable semiconductor, with an indirect bandgap of ~ 0.9 eV and a direct gap of ~ 2.2 eV [6]. ScN thin films with their low resistivity and high Seebeck coefficients lead to a high thermoelectric power factor that makes it a potential candidate for waste-heat-to-electrical energy conversion applications [7]. An extremely high thermoelectric power factor of 3.3– 3.5 mW/m-K^2 at high temperature (500 – 800K) has been demonstrated for ScN thin films deposited on MgO and Al_2O_3 substrates [8]. Such a large power factor of ScN is higher in comparison to the well-known thermoelectric materials such as Be_2Te_3 and La_3Te_4 in a similar temperature range [9,10]. In addition, ScN has been employed to enhance the piezoelectric coefficient in traditional III-nitride compounds such as AlN and GaN [11,12]. Solid-state alloys of $Al_{1-x}Sc_xN$ with Sc concentration up to 43% exhibited five times larger piezoelectric coefficients compared to AlN, and ferroelectricity was demonstrated in $Al_{1-x}Sc_xN$ with Sc concentration of 27% [13,14]. Such features extend the application of ScN-based III-nitride alloys to novel piezoelectric and ferroelectric energy harvesting, bulk, and surface acoustic devices, sensing and switching devices. Furthermore, owing to close matching in-plane lattice parameter of (111) ScN and (0001) GaN, ScN has been used as a buffer layer to reduce the threading dislocation density in GaN epilayer [15,16].

ScN thin films have been deposited using a variety of growth techniques such as hydride vapor phase epitaxy (HVPE)[17], magnetron sputtering [18–22], gas-source and plasma-assisted molecular beam epitaxy [23–26], etc. on a range of substrates such as Si, MgO, Al_2O_3 and SiC to investigate the effects of surface orientation on physical properties. Although epitaxial growth was demonstrated in most of the cases, the surface morphology and electrical transport properties are dependent on the substrate orientation [27]. Since MgO and ScN exhibit rocksalt crystal structure, the ScN thin films deposited on (001) MgO exhibited (001) oriented cubic epitaxial films with smooth surface morphology [19,23]. In some other cases, ScN films deposited on (001) MgO substrates were found to exhibit both (111) and (002) orientations, which is mainly due to growth constraints [19,28]. In contrast, ScN growth on *c*-plane (0001) sapphire, MgO (111), or Si (111) resulted in

* Correspondence to be addressed to
E-mail addresses: bsaha@jncasr.ac.in, bivas.mat@gmail.com (B. Saha).

https://doi.org/10.1016/j.materresbull.2021.111443
Received 30 January 2021; Received in revised form 11 June 2021; Accepted 13 June 2021
Available online 16 June 2021

(111) ScN, while (001) ScN growth was found on *r*-plane sapphire [20,21,25,29]. Such (111) oriented films exhibited columnar growth with (100) facets exposed on the surface.

As-deposited ScN films grown using various techniques are always nearly degenerate with high carrier concentration in the 10^{20} – 10^{21} cm^{-3} range, and resistivity of the order of $\sim 10^{-4}$ Ω-cm at room temperature. Also, the electronic mobility of ScN is found to vary in the range of 50 – 130 cm^2/Vs [6]. The origin of such a high carrier concentration has been attributed to large impurity concentrations such as oxygen and fluorine in ScN that result from the source materials as well as from the process gas during growth [30]. ScN has a high affinity for oxygen, and recent studies have demonstrated oxygen concentration in ScN to be influenced by the growth temperature and crystalline orientations [20]. The large carrier concentration of ScN thin films has been reduced with Mg-acceptor doping and *p*-type ScN thin films that exhibit a large thermoelectric power factor demonstrated [31].

However, to improve the mobility and other electronic properties, low defect density (misfit dislocations, threading dislocations, grain boundaries, etc.) single crystalline ScN thin films need to be developed. As the lattice mismatch between ScN and conventional substrates (001) MgO, 6.4%; (001) Si, 20.6%; (0001)Al_2O_3, 13.9%[24] is quite large, (0001) GaN which exhibits a less than 0.1% lattice-mismatch with (111) ScN, could be utilized as a substrate. In addition, density functional theory calculations have demonstrated that a polarization discontinuity between the (0001) GaN and (111) ScN interfaces can lead to high-density electron or hole gas at the (0001) GaN and (111) ScN interface [32]. In this work, we present (111) oriented lattice-matched ScN film growth on (0001) GaN substrates.

2. Experimental details

ScN thin films were deposited on commercially available MOCVD grown (0001) GaN epilayers on *c*-sapphire substrates. Prior to the growth, the substrates were thoroughly cleaned with organic solvents such as acetone and propanol, followed by a de-ionized water rinse and N_2 blow-drying. For sputter deposition of ScN, a reactive dc magnetron sputtering system (PVD Products, USA) with an ultra-high vacuum chamber at a base pressure of 2×10^{-9} Torr was used. Scandium (99.995% pure) target power was set to 100 W. The Ar (99.99999%) and N_2 (99.99999%) ratio was kept at 9:2 for all the depositions. Before deposition, the substrates were annealed at 750°C for 30 minutes in the growth chamber. The target material Sc was pre-sputtered at actual growth condition for 30 minutes. During deposition, the substrate temperature was maintained at 750°C and the chamber pressure at 5 mTorr.

Post deposition, several ex-situ characterization techniques have been employed to study the samples. A field-emission scanning electron microscope (FESEM, FEI Quanta 3D, Netherlands) was used to study the surface morphology and measure film thickness. High-resolution X-ray diffraction (Bruker, D8 Advance) with Cu Kα radiation (1.5406 Å) was used to determine the structural orientation of the thin films. High-resolution scanning TEM (HRSTEM) imaging, diffraction, and EDS mapping of the samples was performed employing an image and probe-corrected and monochromated FEI Themis-Z instrument equipped with ChemiSTEM EDS detector system for ultrahigh count rates and operated at 300kV.

TEM samples were prepared with a Helios Hydra DualBeam Plasma FIB. Samples were first coated with approximately 20 nm of Au via magnetron sputtering. A 100 nm Pt+C protective cap was deposited inside the FIB with a 5 kV electron beam, followed by a 1 μm Pt+C protective cap with a 12 kV Xe beam. To generate the lamella, samples were trenched with a 30 kV Xe beam at 60, 15 and 4 nA before lift out. The TEM lamellae were welded to Mo grids using ion beam Pt welding. Thinning was done at ±1.5° with currents of 300, 100 pA and 30 kV, using a 5 kV electron beam to check for electron transparency. Final polishing was done with a 5 kV ion beam between 30 and 10 pA. Room temperature electrical properties were measured using Ecopia HMS-3000 tabletop Hall effect measurement system.

3. Results and discussion

The symmetric 2θ - ω X-ray diffractogram of the ScN film shows two prominent peaks at 2θ = 34.5° and 41.72° (Fig. 1(a)). The first peak at 34.5° corresponds to (0002) GaN and (111) ScN. ScN 111 reflection lies within the background of GaN 0002 reflection as the interplanar spacing of (111) ScN planes closely matches with the out-of-plane lattice constant of GaN. This implies that (111) ScN is well aligned with (0001) GaN, i.e., the out-of-plane epitaxial relationship is $(111)_{ScN}\|(0001)_{GaN}$. The peak appearing at 41.72° can be indexed as 0006 reflection from the Al_2O_3 substrate. Since the combined thickness of ScN and GaN is about 3.8 μm, the intensity of the Al_2O_3 substrate peak appear smaller. The full width at half maximum (FWHM) of the rocking curve for the peak at 34.5° (shown in inset Fig. 1a) is found to be about 0.07°. Such a narrow FWHM suggests highly oriented ScN films with negligible out-of-plane misorientation. Fig. 1(b) shows the (002) pole figure of ScN superimposed on that of (101) GaN. The discrete spots are indicative of in-plane epitaxial order in ScN thin film. The pole figure of ScN shows six spots separated by 60° at a tilt angle of 54.2°. The tilt angle corresponds to the angle between (111) and (002) planes of ScN. The presence of six spots instead of three spots (separated by 120°) suggests the existence of two (111) oriented domains rotated by 60° against each other. The twin domains arise due to the symmetric constraint by the three-fold symmetric (111) oriented growth of ScN on six-fold symmetric (0001) GaN. Similar results were obtained for ScN films deposited on other (111) or (0001) oriented substrates [18,33,34]. Similarly, the (101) pole figure of GaN exhibits six spots separated by 60° at a tilt angle of 62°, where the tilt angle corresponds to the angle between (002) and (101) planes of GaN. The appearance of spots corresponding to ScN and GaN at the same azimuthal angle ϕ reveals the in-plane epitaxial relationship as $[002]_{ScN}\|[101]_{GaN}$. Therefore, the overall epitaxial relationship of ScN on GaN is found to be $[002](111)_{ScN}\|\ [101](001)_{GaN}$. This is in contrast to the epitaxial relationship of ScN films deposited on rocksalt (001) MgO substrates that exhibit an epitaxial relationship of $[001](001)_{ScN}\|\ [001](001)_{MgO}$.

The plan-view FESEM image of the ScN thin film shows pyramidal facets (see Fig. 2(a)). Such morphology and texture is typical for (111) ScN grown on (111) MgO and (0001) Al_2O_3 substrates [20,33] and has been attributed to the lower lateral mobility of adatoms on (111) surface in comparison to (001) surface [26,28]. The (111) surface of ScN is expected to have a higher density of dangling bonds, which leads to a higher sticking coefficient for adatoms arriving on the surface. Studies on the temperature dependence of surface roughness in (111) oriented growth of ScN further evidenced the model of limited surface adatom mobility [35]. Further, a closer look at the orientation of the triangular pyramids clearly shows the existence of two kinds of domains. As a guide to the eye, the two domains are marked with red circles (see inset of Fig. 2(a)), which are rotated by 60° with respect to each other. This confirms the results of HRXRD measurements that indicated the presence of (111) oriented twin domains (Fig. 1(b)). The root-mean-square surface roughness for the ScN determined using atomic force microscopy (Fig. 2(b)) was 1.67 nm, representing its smooth epitaxial growth.

The TEM micrograph in cross-section geometry confirms the columnar growth of the ScN film (see Fig. 3(a)). The columns appear rotated in the magnified TEM image (Fig. 3(b)). An arrow and lines are drawn as a guide to the eye to indicate the domain rotation with respect to neighboring columns (inset of**Fig. 3** (b)). The atomic resolution STEM images (c and d) as well as electron diffraction pattern (EDP) analysis (inset of Fig. 3(d)) reveals (111) oriented ScN growth with epitaxial relationship $(110)_{ScN}\|(11\bar{2}0)_{GaN}$ and $[111]_{ScN}\|[0001]_{GaN}$ which is consistent with the HRXRD results. Atomic-resolution HAADF-STEM image along [112] shows (Fig. 3(c) and 3(d)) an atomically sharp and

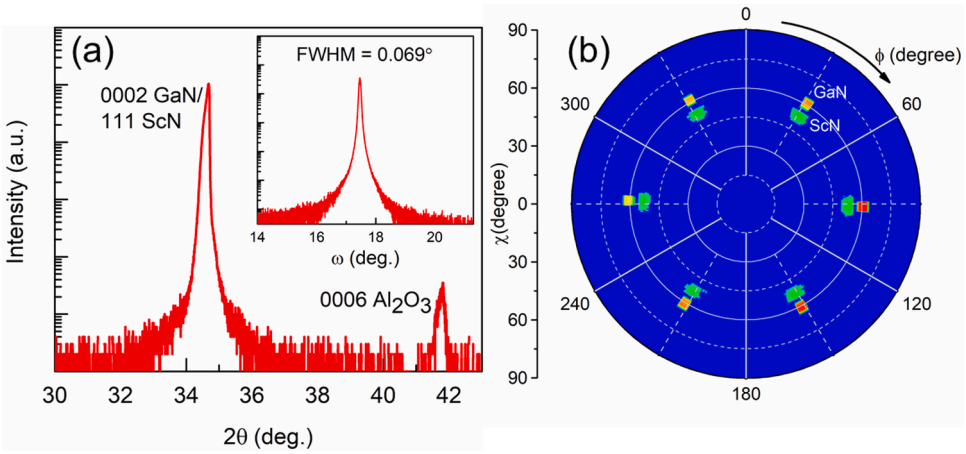

Figure 1. (a) Symmetric 2θ-ω X-ray diffractogram of ScN thin film deposited grown on (0001) GaN substrate. Inset shows ω-scan (rocking curve) corresponding to the 0002 GaN/111 ScN perk. (b) X-ray pole figure of (002) ScN superimposed on that of (101) GaN. Six spots separated by 60° at a tilt angle of 54.2° show the twinned growth of (111) ScN on (0001) GaN.

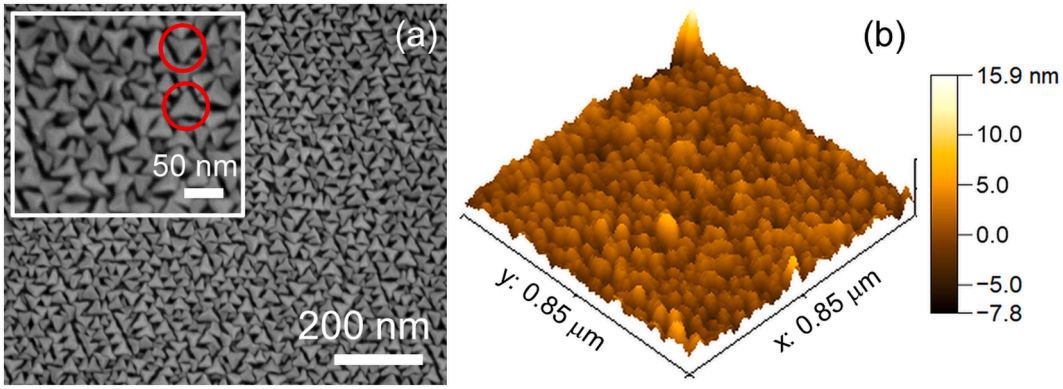

Figure 2. (a) Plan-view FESEM image showing pyramidal (111) oriented ScN growth on (0001) GaN. Red circles in the inset indicate the domains rotated 60° with respect to each other. (b) Atomic force microscopy image of ScN that exhibits a small surface root-mean-square roughness of 1.6 nm.

abrupt ScN/GaN interface. As expected, no misfit dislocation is observed at the interface between ScN and GaN, since the materials are closely lattice-matched. Previous work on the growth of (111) oriented cubic structures on (0001) hexagonal surface had suggested domain matching epitaxy under suitable conditions [36,37]. Such type of growth can lead to pyramidal domains (as seen in FESEM image Fig. 2(a)) without any misfit dislocations [38]. From Fig. 3(c), the growth near the interface occurs in a layer-by-layer mode, which transitions to a columnar mode as growth proceeds. HRSTEM energy dispersive X-ray spectroscopy (EDS) elemental mapping shows (Fig. 4) uniform distribution of Sc and N throughout the film. It also shows the presence of oxygen in ScN film that typically arises from target contamination or process gas during the film growth.

Theoretically, several types of twinned domains are possible in an fcc lattice. However, we find only the rotational type of twinning (with [111] rotational axis) in the present case. As mentioned above, a similar kind of rotational twinning was observed in several other hetero-epitaxial systems, even in the case of close lattice matching [36,37,39]. It can be noted that while the (111) ScN and (0001) GaN exhibit close lattice matching in the plane forming the interface, they comprise a mismatch in rotational symmetry. As a consequence, rotational twin domains will form in the ScN thin films [40]. Based on group theory, it was predicted that an epilayer with threefold rotational symmetry on a substrate with sixfold rotational symmetry could have a minimum of two rotational domains with in-plane rotation about the substrate normal [41]. In addition, the substrate surface, i.e., the first layer or first two layers (surface reconstruction), can have a different symmetry than that of the bulk [42]. Thus, depending on whether the adatoms of the growing film interacts with the surface or a lower layer of the substrate, domains with two different orientations can nucleate. Similarly, steps (separating atomically flat terraces) on the substrate surface, which are quite common in practical cases, can offer identical or different crystallographic orientation depending on the step height. For the wurtzite (0001) GaN surface, a step height of c/2 offers an identical surface with 180° rotated orientation [42]. In the literature, the formation of twinned domains during epitaxial growth has been attributed to a variety of growth parameters. In the case of (111) CdTe/ (0001) Al_2O_3, the formation of rotational twin domains was attributed to the termination of sapphire surface as it plays a crucial role in determining whether the growth initiated with a Cd or Te layer [43,44]. Studies on (111) SiGe alloy growth on (0001) sapphire has shown that the formation of twin domains is dependent on the substrate temperature [36,39]. The ScN films in this study are grown at a homologous temperature higher than 0.3, which we have recently shown will result in nominally single-crystalline ScN [45]. However, it should be noted that the films are grown on commercially available MOCVD grown GaN epilayers on *c*-sapphire substrates. Figure 5 shows a cross-sectional TEM image of the GaN epilayer and *c*-sapphire interface as well as the GaN and ScN interface. The interface between the GaN and sapphire is found to have a high density of defects (Fig. 5(a)), from which dislocations run vertically through the GaN epilayers. A large number of such dislocations terminate at the GaN surface. One such dislocation line extending through the

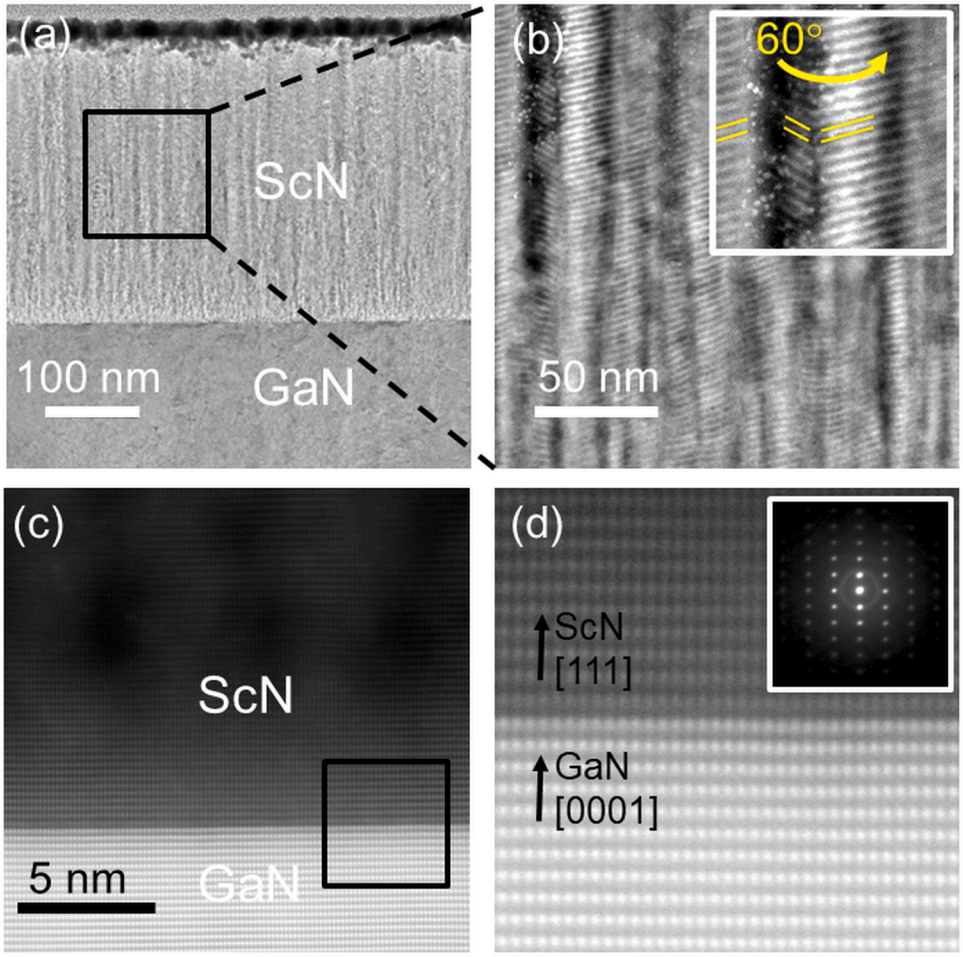

Figure 3. (a) Cross-sectional TEM image of ScN thin film deposited on (0001) GaN surface showing columnar grain growth. (b) Magnified image of the ScN columns (the part marked with a black square in (a)). Twin domains rotated by 60° along [111] are indicated in the inset. (c) Atomic resolution HAADF STEM image of the ScN and GaN interface along the ScN [112] zone axis. (d) Magnified interface region between ScN/GaN marked with black square (in (c)) with inset showing corresponding selected area diffraction pattern of ScN.

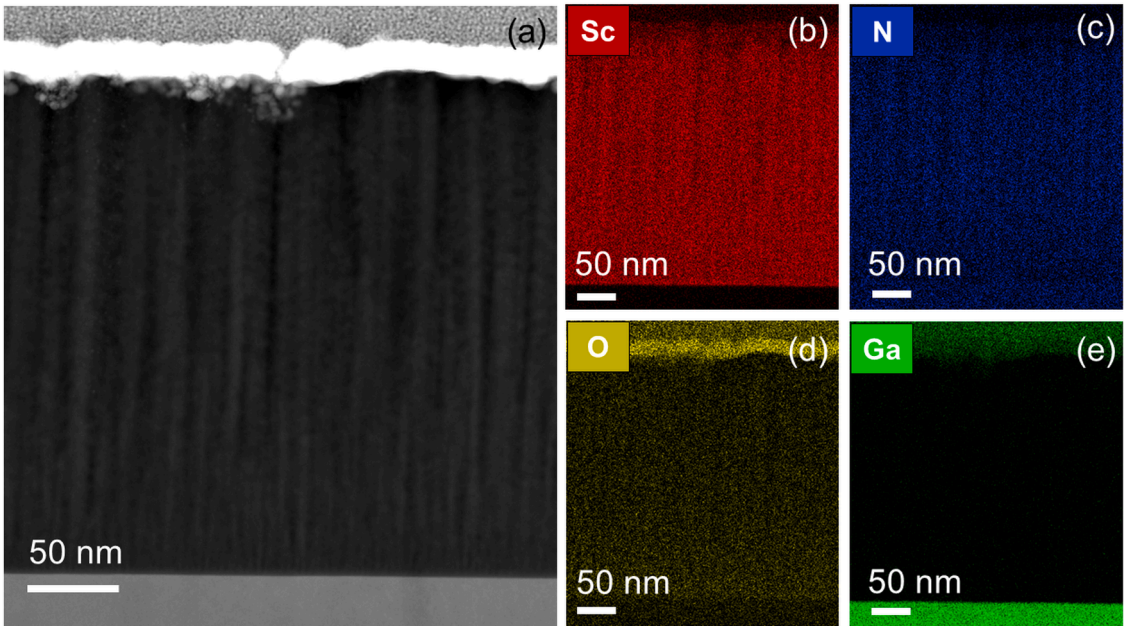

Figure 4. (a) HAADF-STEM image of ScN deposited on the (0001) GaN substrate showing columnar growth. Respective STEM-EDS maps of Sc (b), N (c), O (d) as well as Ga (e). No inter-diffusion of Ga was observed.

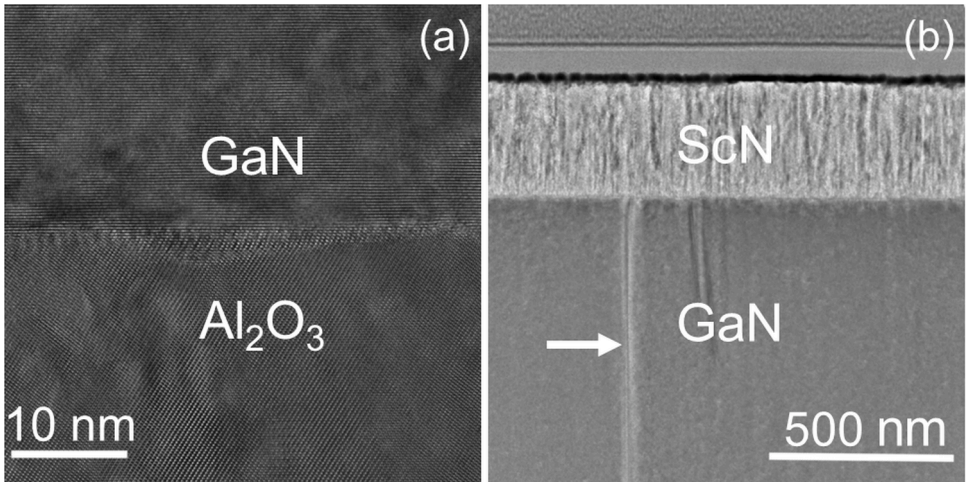

Figure 5. Cross-sectional TEM image of the Al_2O_3/GaN interface revealing regions of high defect density (a), and GaN/ScN interface (b). A dislocation line is indicated with an arrow, which originates at the Al_2O_3/GaN interface and extends through the entire GaN epilayer terminating at the GaN/ScN interface.

GaN epilayer towards the GaN/ScN interface is shown in Fig. 5(b). Hence, surface termination of the dislocations and resulting defects at the GaN/ScN interface can contribute to twin domain formation in the (111) ScN thin films.

Room-temperature Hall measurements were performed on (111) ScN samples in van der Pauw geometry. The samples exhibited high hall mobility ranging 124 – 177 cm^2/Vs with a corresponding *n*-type carrier concentration of 1.05 × 10^{18} cm^{-3} and the resistivity of 48.1 mΩ-cm. The mobility obtained here is higher than the typical values reported for ScN growth on MgO or sapphire substrates but is slightly lower than HVPE grown ScN, which exhibited the highest mobility value of up to 284 cm^2/Vs to date. Also, the measured carrier concentration was two orders of magnitude lower than that of undoped ScN thin films deposited on other substrates. Such high mobility and low carrier concentration can be the possible outcome of a significant reduction in misfit defects and threading dislocations due to the close in-plane lattice-matched growth of ScN on the (0001) GaN surface. In an ionic crystal, such extended defects are expected to be charged and electrically active and act as scattering centers. Further, these results are in line with the speculations made by Dismukes et al. and Oshima et al. that reducing defects in ScN films can result in carrier concentrations as low as 10^{18} cm^{-3} and mobility close to that of Ge and Si [17,46].

4. Conclusions

Highly (111) oriented ScN thin films are deposited on lattice-matched *c*-plane GaN surface. Structural analysis indicated that growth on **a** hexagonal substrate with (0001) oriented surface led to (111) oriented columnar growth of ScN instead of (001) ScN. The HRXRD analysis revealed an epitaxial relationship of $[111]_{ScN}\|[0001]_{GaN}$. The analysis of the (002) pole figure clearly showed the presence of two (111) oriented domains, with one of the domains rotated by 60° to accommodate the sixfold symmetry of the substrate. TEM analysis reveals dislocations originating at the Al_2O_3/GaN interface and vertically extending throughout the GaN film to its interface with ScN as a possible cause for the twinning. Within the individual domains, however, high-resolution STEM images of the interface demonstrate the absence of misfit dislocations over distances of tens of nanometers due to the near-perfect lattice match of ScN [111] with the GaN [0001] substrate. This has a significant effect on the electrical transport properties of the ScN thin films. Room temperature electrical measurements revealed high hall mobility of 177 cm^2/Vs in comparison to previously reported values for ScN. Demonstration of single-crystal ScN growth on GaN with reduced interfacial defects marks important progress in ScN research. This is expected to improve the transport properties and make novel electronic device application of ScN possible.

Author Statement

Shashidhara Acharya: Investigation, Data curation, Methodology, Software, Writing-Original draft preparation, **Abhijit Chatterjee**: Investigation, Writing- Reviewing and Editing. **Vijay Bhatia:** Visualization, Investigation, Writing-Reviewing and Editing, **Ashalatha Indiradevi Kamalasanan Pillai**: Visualization, Investigation, **Magnus Garbrecht**: Investigation, Writing- Reviewing and Editing. **Bivas Saha:** Conceptualization, Investigation, Supervision, Writing- Reviewing and Editing.

Declaration of Competing Interest

The authors declare that they have no known competing financial interests or personal relationships that could have appeared to influence the work reported in this paper.

Acknowledgements

SA and BS acknowledge support from the International Centre for Materials Science and Sheikh Saqr Laboratory of the Jawaharlal Nehru Centre for Advanced Scientific Research. BS acknowledge Young Scientist Research Award (YSRA) from the Board of Research in Nuclear Sciences (BRNS), Department of Atomic Energy (DAE), India with grant number 59/20/10/2020-BRNS/59020 for financial support. The authors acknowledge the facilities of Sydney Microscopy and Microanalysis at The University of Sydney. The authors acknowledge the facilities of Sydney Microscopy and Microanalysis at The University of Sydney.

References

[1] K.V. Chauhan, S.K. Rawal, A Review Paper on Tribological and Mechanical Properties of Ternary Nitride based Coatings, Procedia Technol 14 (2014) 430–437, https://doi.org/10.1016/j.protcy.2014.08.055.
[2] B. Saha, S.K. Lawrence, J.L. Schroeder, J. Birch, D.F. Bahr, T.D. Sands, Enhanced hardness in epitaxial TiAlScN alloy thin films and rocksalt TiN/(Al,Sc)N superlattices, Appl. Phys. Lett. 105 (2014), 151904, https://doi.org/10.1063/1.4898067.
[3] B. Saha, A. Shakouri, T.D. Sands, Rocksalt nitride metal/semiconductor superlattices: A new class of artificially structured materials, Appl. Phys. Rev. 5 (2018) 1–56, https://doi.org/10.1063/1.5011972.
[4] G.V. Naik, V.M. Shalaev, A. Boltasseva, Alternative plasmonic materials: Beyond gold and silver, Adv. Mater. 25 (2013) 3264–3294, https://doi.org/10.1002/adma.201205076.

[5] W. Li, U. Guler, N. Kinsey, G.V. Naik, A. Boltasseva, J. Guan, V.M. Shalaev, A. V. Kildishev, Refractory plasmonics with titanium nitride: Broadband, Adv. Mater. 26 (2014) 7959–7965, https://doi.org/10.1002/adma.201401874.

[6] B. Biswas, B. Saha, Development of semiconducting ScN, Phys. Rev. Mater. 3 (2019) 1–25, https://doi.org/10.1103/PhysRevMaterials.3.020301.

[7] P. Eklund, S. Kerdsongpanya, B. Alling, Transition-metal-nitride-based thin films as novel energy harvesting materials, J. Mater. Chem. C. 4 (2016) 3905–3914, https://doi.org/10.1039/c5tc03891j.

[8] P.V. Burmistrova, J. Maassen, T. Favaloro, B. Saha, S. Salamat, Y. Rui Koh, M. S. Lundstrom, A. Shakouri, T.D. Sands, Thermoelectric properties of epitaxial ScN films deposited by reactive magnetron sputtering onto MgO(001) substrates, J. Appl. Phys. 113 (2013), 153704, https://doi.org/10.1063/1.4801886.

[9] J.R. Sootsman, D.Y. Chung, M.G. Kanatzidis, New and old concepts in thermoelectric materials, Angew. Chemie - Int. Ed. 48 (2009) 8616–8639, https://doi.org/10.1002/anie.200900598.

[10] L. Gao, J. Zhu, H. Wang, F. Ren, B. Zhao, Study on the effect of Pb partial substitution for Te on the thermoelectric properties of La 3Te 4-xPb x materials, J. Phys. D. Appl. Phys. 45 (2012), https://doi.org/10.1088/0022-3727/45/18/185303.

[11] D. Jena, R. Page, J. Casamento, P. Dang, J. Singhal, Z. Zhang, J. Wright, G. Khalsa, Y. Cho, H.G. Xing, The new nitrides: Layered, ferroelectric, magnetic, metallic and superconducting nitrides to boost the GaN photonics and electronics eco-system, Jpn. J. Appl. Phys. 58 (2019), https://doi.org/10.7567/1347-4065/ab147b.

[12] M.A. Moram, S. Zhang, ScGaN and ScAlN: Emerging nitride materials, J. Mater. Chem. A. 2 (2014) 6042–6050, https://doi.org/10.1039/c3ta14189f.

[13] M. Akiyama, T. Kamohara, K. Kano, A. Teshigahara, Y. Takeuchi, N. Kawahara, Enhancement of piezoelectric response in scandium aluminum nitride alloy thin films prepared by dual reactive cosputtering, Adv. Mater. 21 (2009) 593–596, https://doi.org/10.1002/adma.200802611.

[14] S. Fichtner, N. Wolff, F. Lofink, L. Kienle, B. Wagner, AlScN: A III-V semiconductor based ferroelectric, J. Appl. Phys. 125 (2019), https://doi.org/10.1063/1.5084945.

[15] M.A. Moram, Y. Zhang, M.J. Kappers, Z.H. Barber, C.J. Humphreys, Dislocation reduction in gallium nitride films using scandium nitride interlayers, Appl. Phys. Lett. 91 (2007) 89–92, https://doi.org/10.1063/1.2794009.

[16] L. Lupina, M.H. Zoellner, T. Niermann, B. Dietrich, G. Capellini, S.B. Thapa, M. Haeberlen, M. Lehmann, P. Storck, T. Schroeder, Zero lattice mismatch and twin-free single crystalline ScN buffer layers for GaN growth on silicon, Appl. Phys. Lett. 107 (2015), https://doi.org/10.1063/1.4935856.

[17] J.P. Dismukes, W.M. Yim, V.S. Ban, Epitaxial growth and properties of semiconducting ScN, J. Cryst. Growth. 13–14 (1972) 365–370, https://doi.org/10.1016/0022-0248(72)90185-6.

[18] S. Kerdsongpanya, N. Van Nong, N. Pryds, A. Žukauskaitė, J. Jensen, J. Birch, J. Lu, L. Hultman, G. Wingqvist, P. Eklund, Anomalously high thermoelectric power factor in epitaxial ScN thin films, Appl. Phys. Lett. 99 (2011), 232113, https://doi.org/10.1063/1.3665945.

[19] D. Gall, I. Petrov, L.D. Madsen, J.-E. Sundgren, J.E. Greene, Microstructure and electronic properties of the refractory semiconductor ScN grown on MgO(001) by ultra-high-vacuum reactive magnetron sputter deposition, J. Vac. Sci. Technol. A Vacuum, Surfaces, Film. 16 (1998) 2411–2417, https://doi.org/10.1116/1.581360.

[20] A. le Febvrier, N. Tureson, N. Stilkerich, G. Greczynski, P. Eklund, Effect of impurities on morphology, growth mode, and thermoelectric properties of (1 1 1) and (0 0 1) epitaxial-like ScN films, J. Phys. D. Appl. Phys. 52 (2019), 035302, https://doi.org/10.1088/1361-6463/aaeb1b.

[21] J.M. Gregoire, S.D. Kirby, G.E. Scopelianos, F.H. Lee, R.B. Van Dover, High mobility single crystalline ScN and single-orientation epitaxial YN on sapphire via magnetron sputtering, J. Appl. Phys. 104 (2008), https://doi.org/10.1063/1.2996006.

[22] S. Kerdsongpanya, O. Hellman, B. Sun, Y.K. Koh, J. Lu, N. Van Nong, S.I. Simak, B. Alling, P. Eklund, Phonon thermal conductivity of scandium nitride for thermoelectrics from first-principles calculations and thin-film growth, Phys. Rev. B. 96 (2017) 1–6, https://doi.org/10.1103/PhysRevB.96.195417.

[23] D. Rao, B. Biswas, E. Flores, A. Chatterjee, M. Garbrecht, Y.R. Koh, V. Bhatia, A.I. K. Pillai, P.E. Hopkins, M. Martin-Gonzalez, B. Saha, High mobility and high thermoelectric power factor in epitaxial ScN thin films deposited with plasma-assisted molecular beam epitaxy, Appl. Phys. Lett. 116 (2020), https://doi.org/10.1063/5.0004761.

[24] S.W. King, R.F. Davis, R.J. Nemanich, Gas source molecular beam epitaxy of scandium nitride on silicon carbide and gallium nitride surfaces, J. Vac. Sci. Technol. A Vacuum, Surfaces, Film. 32 (2014), 061504, https://doi.org/10.1116/1.4894816.

[25] T. Ohgaki, K. Watanabe, Y. Adachi, I. Sakaguchi, S. Hishita, N. Ohashi, H. Haneda, Electrical properties of scandium nitride epitaxial films grown on (100) magnesium oxide substrates by molecular beam epitaxy, J. Appl. Phys. 114 (2013) 93704, https://doi.org/10.1063/1.4820391.

[26] A.R. Smith, H.A.H. Al-Brithen, D.C. Ingram, D. Gall, Molecular beam epitaxy control of the structural, optical, and electronic properties of ScN(001), J. Appl. Phys. 90 (2001) 1809–1816, https://doi.org/10.1063/1.1388161.

[27] T. Ohgaki, I. Sakaguchi, N. Ohashi, H. Haneda, Heteroepitaxial growth and electric properties of (110)-oriented scandium nitride films, J. Cryst. Growth. 476 (2017) 12–16, https://doi.org/10.1016/j.jcrysgro.2017.08.002.

[28] D. Gall, I. Petrov, N. Hellgren, L. Hultman, J.E. Sundgren, J.E. Greene, Growth of poly- and single-crystal ScN on MgO(001): Role of low-energy N+2 irradiation in determining texture, microstructure evolution, and mechanical properties, J. Appl. Phys. 84 (1998) 6034–6041, https://doi.org/10.1063/1.368913.

[29] T. Ohgaki, I. Sakaguchi, N. Ohashi, Structure and electron mobility of ScN films grown on α-Al2O3(1102) substrates, Materials 11 (2018) 22–25, https://doi.org/10.3390/ma11122449.

[30] J.S. Cetnar, A.N. Reed, S.C. Badescu, S. Vangala, H.A. Smith, D.C. Look, Electronic transport in degenerate (100) scandium nitride thin films on magnesium oxide substrates, Appl. Phys. Lett. 113 (2018), https://doi.org/10.1063/1.5050200.

[31] B. Saha, M. Garbrecht, J.A. Perez-Taborda, M.H. Fawey, Y.R. Koh, A. Shakouri, M. Martin-Gonzalez, L. Hultman, T.D. Sands, Compensation of native donor doping in ScN: Carrier concentration control and p-type ScN, Appl. Phys. Lett. 110 (2017) 1–6, https://doi.org/10.1063/1.4989530.

[32] N.L. Adamski, C.E. Dreyer, C.G. Van de Walle, Giant polarization charge density at lattice-matched GaN/ScN interfaces, Appl. Phys. Lett. 115 (2019), 232103, https://doi.org/10.1063/1.5126717.

[33] M.A. Moram, T.B. Joyce, P.R. Chalker, Z.H. Barber, C.J. Humphreys, Microstructure of epitaxial scandium nitride films grown on silicon, Appl. Surf. Sci. 252 (2006) 8385–8387, https://doi.org/10.1016/j.apsusc.2005.11.069.

[34] J. Casamento, J. Wright, R. Chaudhuri, H. Xing, D. Jena, Molecular beam epitaxial growth of scandium nitride on hexagonal SiC, GaN, and AlN, Appl. Phys. Lett. 115 (2019), 172101, https://doi.org/10.1063/1.5121329.

[35] M.A. Moram, Z.H. Barber, C.J. Humphreys, T.B. Joyce, P.R. Chalker, Young's modulus, Poisson's ratio, and residual stress and strain in (111)-oriented scandium nitride thin films on silicon, J. Appl. Phys. 100 (2006) 1–6, https://doi.org/10.1063/1.2217106.

[36] H.J. Kim, H. Bin Bae, Y. Park, K. Lee, S.H. Choi, Temperature dependence of crystalline SiGe growth on sapphire (0001) substrates by sputtering, J. Cryst. Growth. 353 (2012) 124–128, https://doi.org/10.1016/j.jcrysgro.2012.05.009.

[37] Y. Park, M.J. Cich, R. Zhao, P. Specht, E.R. Weber, E. Stach, S. Nozaki, Analysis of twin defects in GaAs(111)B molecular beam epitaxy growth, J. Vac. Sci. Technol. B Microelectron. Nanom. Struct. 18 (2000) 1566, https://doi.org/10.1116/1.591427.

[38] H.J. Kim, A. Duzik, S.H. Choi, Lattice-alignment mechanism of SiGe on Sapphire, Acta Mater 145 (2018) 1–7, https://doi.org/10.1016/j.actamat.2017.11.031.

[39] Y. Park, G.C. King, S.H. Choi, Rhombohedral epitaxy of cubic SiGe on trigonal c -plane sapphire, 310 (2008) 2724–2731. doi:10.1016/j.jcrysgro.2008.02.010.

[40] R.C. Pond, Crystallography of domain formation and dislocations in bilayers and multilayers, Crit. Rev. Solid State Mater. Sci. 15 (1989) 441–472, https://doi.org/10.1080/10408438908243742.

[41] M. Lorenz, M. Grundmann, T. Bo, Occurrence of Rotation Domains in Heteroepitaxy, 146102 (2010) 1–4. doi:10.1103/PhysRevLett.105.146102.

[42] M. Grundmann, Formation of epitaxial domains: Unified theory and survey of experimental results, Phys. Status Solidi. 248 (2011) 805–824, https://doi.org/10.1002/pssb.201046530.

[43] S. Neretina, R.A. Hughes, J.F. Britten, N.V. Sochinskii, J.S. Preston, P. Mascher, The role of substrate surface termination in the deposition of (111) CdTe on (0001) sapphire, Appl. Phys. A Mater. Sci. Process. 96 (2009) 429–433, https://doi.org/10.1007/s00339-009-5285-0.

[44] J. Zúñiga-Pérez, R. Tena-Zaera, V. Muñoz-Sanjosé, Structural characterization of CdTe layers grown on (0 0 0 1) sapphire by MOCVD, J. Cryst. Growth. 270 (2004) 309–315, https://doi.org/10.1016/j.jcrysgro.2004.06.043.

[45] D. Rao, B. Biswas, S. Acharya, V. Bhatia, A.I.K. Pillai, M. Garbrecht, B. Saha, Effects of adatom mobility and Ehrlich–Schwoebel barrier on heteroepitaxial growth of scandium nitride (ScN) thin films, Appl. Phys. Lett. 117 (2020), 212101, https://doi.org/10.1063/5.0027091.

[46] Y. Oshima, E.G. Villora, K. Shimamura, Hydride vapor phase epitaxy and characterization of high-quality ScN epilayers, J. Appl. Phys. 115 (2014), https://doi.org/10.1063/1.4871656.